Available online at www.sciencedirect.com
SCIENCE DIRECT
Journal of Magnetic Resonance 180 (2006) 118–126
JMR Journal of Magnetic Resonance
www.elsevier.com/locate/jmr

Multiexponential attenuation of the CPMG spin echoes due to a geometrical confinement

D.S. Grebenkov *

Unité de Recherche en Résonance Magnétique Médicale, Université Paris-Sud XI – C.N.R.S. UMR 8081, 91405 Orsay, France

Received 31 October 2005; revised 3 January 2006
Available online 17 February 2006

Abstract

The CPMG multi-echo technique is often used to investigate the translational motion of diffusing nuclei in a confining medium. Henceforth, periodically repeated RF pulses with a diffusion-sensitizing gradient yield a formation of spin echoes of gradually decreasing amplitudes. The parameters of their exponential fits may characterize the structure of porous materials or biological tissue. In this paper, a multiexponential character of the CPMG measurements is rigorously demonstrated, once a geometrical confinement is present. Based on the multiple propagator approach, we derived a spectral representation for the echo amplitudes under external magnetic field of an arbitrary gradient profile. The multiple relaxation times and their spectral weights were found in a general form. The study of simple restrictive media allowed to obtain a quantitative condition under which the multiexponential attenuation is reduced to a monoexponential one.

Keywords: Magnetic resonance; Multi-echo; CPMG; Restricted diffusion; Confined media; Multiexponential behavior

1. Introduction

The pulsed gradient spin echo technique is widely applied to study the confinement of diffusing particles in restricted geometry [1]. The use of the time-depended magnetic field gradient to encode the spin phase distribution for translational motion of nuclei provides a mean to characterize complex structures like porous materials or biological tissues [2–10].

In the multi-echo or Carr–Purcell–Meiboom–Gill (CPMG) technique, a first 90° RF pulse flips the spin magnetization into the transverse plane. Periodic repetition of a 180° RF pulse with diffusion-sensitizing gradients yields progressive signal attenuation due to intrinsic spin–spin relaxation and to translational motion of the nuclei (Fig. 1). In the case of free diffusion under a steady gradient of amplitude g, a *monoexponential* attenuation has been demonstrated in [11,12]

$$S(nT) \propto \exp(-nT/T_{\mathrm{cpmg}}) \tag{1}$$

with the characteristic relaxation time T_{cpmg}

$$\frac{1}{T_{\mathrm{cpmg}}} = \frac{1}{T_2} + \frac{D\gamma^2 g^2 T^2}{12}, \tag{2}$$

where T_2 is the intrinsic spin–spin relaxation time, D is the (free) self-diffusion coefficient, T is the echo time, and γ is the nuclear gyromagnetic ratio. This behavior has been thoroughly verified in experiments (see [1] and references therein). In this case, a few experimental values $S(nT)$, two at least, are sufficient to compute the relaxation time T_{cpmg} as

$$\frac{1}{T_{\mathrm{cpmg}}} \simeq \frac{1}{T} \ln\left[\frac{S(nT)}{S((n+1)T)}\right], \tag{3}$$

which does not depend on the echo number n. It allows one to find the diffusion coefficient D or spin–spin relaxation time T_2 quite accurately [1]. Relatively simple implementation

* Fax: +39 081 676346.
E-mail address: denis.grebenkov@polytechnique.edu.

1090-7807/$ - see front matter © 2006 Elsevier Inc. All rights reserved.
doi:10.1016/j.jmr.2006.01.014

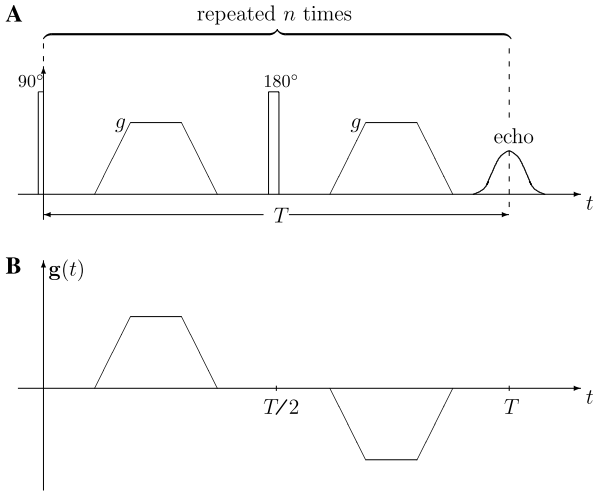

Fig. 1. (A) Typical CPMG sequence starts with a 90° RF pulse followed by periodic repetition of a 180° RF pulse with diffusion-sensitizing gradients (e.g., of trapezoidal shape). The pulsed gradient profile is supposed to be the same before and after 180° RF pulse. The phase cycling of the 180° RF pulses can be applied to reduce the adverse effects of RF inhomogeneities [26]. (B) Effective gradient profile $\mathbf{g}(t)$ accounts for the inversion of the magnetization orientation by the 180° RF pulse as change of the gradient direction.

of CPMG sequences made them a powerful experimental tool to investigate the diffusive motion in natural or artificial structures, e.g., porous structure of rocks [13], cements [14–17], or alveolar tissues of the human lungs [18].

However, the restrictive character of the motion in such complex geometry may modify not only the diffusion coefficient (as a result of tortuosity effect in porous materials [19–24]), but, more importantly, the monoexponential attenuation of the signal [25]. This point can be illustrated by a simple case. For slow diffusion, only a small fraction of nuclei can reach the boundaries during the short echo time T. One could thus expect that the relation (1) still holds, at least for the first echoes. However, with a further increase of the echo number, larger and larger fractions of nuclei encounter the boundaries. For n large enough, the interfacial confinement affects the Brownian motion so strongly that the free diffusion regime and relation (1) become invalid. In particular, one may expect a passage to the fast diffusion limit for very large echo numbers. In this light, several theoretical questions appear: what type of behavior has to be expected, how many characteristic times may be involved, what is the role of a geometrical confinement, where such different situations can be experimentally observed?

The goal of this paper was to provide rigorous responses to these fundamental questions. For this purpose, we first derive a formal spectral representation of the signal based on the multiple propagator approach [27,28]. We demonstrate that once the diffusive motion is geometrically restricted, *multiexponential* attenuation of the CPMG echo train occurs. The involved characteristic times and their weights are then related to the spectral parameters. From the numerical study of typical restrictive domains (two planes, cylinder, and sphere), we define simple conditions under which the multiexponential behavior is reduced to a monoexponential one.

2. Multiple propagator approach

Although the spin echo phenomenology is relatively well understood, the theoretical and numerical NMR study of restricted diffusion in irregular domains still presents a challenging issue. Considerable progress has been achieved by the *multiple propagator approach* first proposed by Caprihan et al. [27], further developed by Callaghan [28] and equivalently reformulated by Barzykin [29,30] and Sukstanskii and Yablonskiy [31].

Let us consider the diffusive motion of a nucleus between the first 90° RF pulse and the moment T of echo formation, in presence of a linear time-dependent gradient of the magnetic field (an example of trapezoidal gradient shape is shown in Fig. 1A). Throughout this paper, the effect of residual magnetic field inhomogeneities is neglected, i.e., the diffusion-sensitizing gradient only can lead to the nuclei dephasing (perfect shimming of the system, no susceptibility effect, etc.). The application of the 180° RF pulse can be taken into account through an effective gradient profile $\mathbf{g}(t)$ for which the magnetization direction is inverted after $T/2$ (Fig. 1B). Since gradients before and after 180° RF pulse are supposed to be identical, the effective gradient profile $\mathbf{g}(t)$ is antisymmetric with respect to the time $T/2$:

$$\mathbf{g}(T-t) = -\mathbf{g}(t). \tag{4}$$

In particular, the *rephasing condition* required for echo formation is automatically satisfied,

$$\int_0^T \mathrm{d}t\ \mathbf{g}(t) = 0, \tag{5}$$

i.e., the accumulated phase φ of an immobile nucleus is strictly zero. In other words, the diffusive motion only has to be responsible for nuclei dephasing and the consequent signal attenuation. We do not consider here the intrinsic spin–spin relaxation also leading to the signal attenuation since it can be easily taken into account as in Eq. (2).

According to the multiple propagator approach, the phase accumulated by a diffusing particle during its stochastic motion under magnetic field is equal to

$$\varphi = \gamma \int_0^T \mathrm{d}t\ (\mathbf{g}(t)\cdot\mathbf{r}(t)),$$

where $(\mathbf{g}(t)\cdot\mathbf{r}(t))$ denotes the scalar product between the effective gradient $\mathbf{g}(t)$ and the position $\mathbf{r}(t)$ of the diffusing nucleus at time t. Dividing the time interval $[0,T]$ into N

subintervals of duration $\tau = T/N$, one uses the trapezoidal approximation of the integral to get

$$\varphi \simeq \gamma \sum_{k=0}^{N-1} \tau \frac{(\mathbf{g}(k\tau+\tau)\cdot\mathbf{r}(k\tau+\tau)) + (\mathbf{g}(k\tau)\cdot\mathbf{r}(k\tau))}{2}.$$

If the time step τ is small enough, the factor 1/2 in front of the first and the last terms can be neglected in order to write the accumulated phase in a simpler form:

$$\varphi \simeq \tau\gamma \sum_{k=0}^{N} (\mathbf{g}(k\tau)\cdot\mathbf{r}(k\tau)). \tag{6}$$

The contribution $e^{i\varphi}$ of one nucleus to the entire signal has to be averaged over the whole ensemble. The initial position $\mathbf{r}_0$ of a nucleus in the confining domain Ω is distributed according to a given steady-state density $\rho(\mathbf{r}_0)$. The probability distribution of the position $\mathbf{r}_1 = \mathbf{r}(\tau)$ after time τ is defined by the Green function $G_\tau(\mathbf{r}_0, \mathbf{r}_1)$ of the diffusion operator. This function, also called *propagator*, is a solution of the diffusion equation in the domain Ω

$$\left[\frac{\partial}{\partial t} - D\Delta\right] G_t(\mathbf{r}, \mathbf{r}') = \delta(\mathbf{r}-\mathbf{r}')\delta(t),$$

where $\delta(\cdot)$ is the Dirac delta-function (distribution). If the interface is impermeable for nuclei and does not contain magnetic impurities which may lead to surface relaxation, the Neumann (or reflecting) boundary condition is imposed. We focus our attention on this specific case, bearing in mind that an extension to a more general mixed boundary condition is straightforward (see [30,32] for details).

The Markovian property of the Brownian motion ensures that, once arrived at position $\mathbf{r}_1$, the distribution of the next position $\mathbf{r}_2 = \mathbf{r}(2\tau)$ is again given by the Green function $G_\tau(\mathbf{r}_1, \mathbf{r}_2)$. Repeatedly applying this property, one obtains the signal at time $T = N\tau$ as

$$S(T) = \int_\Omega d\mathbf{r}_0 \int_\Omega d\mathbf{r}_1 \cdots \int_\Omega d\mathbf{r}_n \rho(\mathbf{r}_0)\, e^{i\gamma\tau(\mathbf{r}_0\cdot\mathbf{g}(0))} \times G_\tau(\mathbf{r}_0, \mathbf{r}_1)\, e^{i\gamma\tau(\mathbf{r}_1\cdot\mathbf{g}(\tau))} G_\tau(\mathbf{r}_1, \mathbf{r}_2) \cdots e^{i\gamma\tau(\mathbf{r}_N\cdot\mathbf{g}(N\tau))}. \tag{7}$$

In this expression, the Green functions encode stochastic motion during successive time intervals of duration τ, while exponential factors represent "elementary" variations of the nucleus phase.

To proceed further, a spectral decomposition of the Green function $G_\tau(\mathbf{r}, \mathbf{r}')$ over the eigenfunctions $u_m(\mathbf{r})$ of the Laplace operator Δ in the domain Ω is used[1]:

$$G_\tau(\mathbf{r}, \mathbf{r}') = \sum_m u_m(\mathbf{r})\; u_m^*(\mathbf{r}')\, e^{-\kappa_m \tau},$$

κ_m being eigenvalues of the Laplace operator [33]. After substitution of this decomposition for the Green functions in (7), summation over each index m is thought as a matrix product. In this way, Callaghan derived a convenient matrix representation of the entire signal for an arbitrary gradient profile $\mathbf{g}(t)$ [28]. In our notation, the signal at time T is equal to scalar product between two vectors, U and HU^*,

$$S(T) = (U \cdot HU^*), \tag{8}$$

where the asterisk denotes complex conjugate. The infinite-dimension vector U is composed of the Fourier transforms of eigenfunctions $u_m(\mathbf{r})$

$$U_m = V^{-1/2} \int_\Omega d\mathbf{r}\; u_m(\mathbf{r}) \exp[i\gamma\tau(\mathbf{r}\cdot\mathbf{g}(0))], \tag{9}$$

while infinite-dimension matrix H is determined by the effective gradient profile $\mathbf{g}(t)$ as product

$$H = RA(\gamma\tau\mathbf{g}(\tau))\; R \cdots A(\gamma\tau\mathbf{g}(n\tau-\tau))R. \tag{10}$$

Here two infinite-dimension matrices R and A represent the "elementary" stochastic displacement and the "elementary" phase variations, respectively, with

$$R_{m,m'} = \delta_{m,m'} \exp[-\kappa_m \tau], \tag{11}$$

$$A_{m,m'}(\mathbf{q}) = \int_\Omega d\mathbf{r}\; u_m^*(\mathbf{r}) u_{m'}(\mathbf{r}) \exp[i(\mathbf{r}\cdot\mathbf{q})]. \tag{12}$$

The multiple propagator approach had been successfully applied to study the restricted diffusion between two parallel planes (one-dimensional restriction), inside an infinite cylinder (2D), and inside a sphere (3D), when the eigenfunctions $u_m(\mathbf{r})$ are known in an explicit analytical form [31,32]. Although the shape of these domains is quite simple, their use to model a geometrical confinement was fruitful for a better understanding of the diffusive motion in more realistic media.

3. Spectral representation

From a mathematical point of view, the condition (4) implies that the matrix H is Hermitian, i.e., $H_{jk}^* = H_{kj}$, so its eigenvalues λ_α and eigenvectors V_α can be introduced as:

$$HV_\alpha = \lambda_\alpha V_\alpha.$$

The scalar product in (8) can thus be written in the *spectral decomposition*

$$S(T) = \sum_\alpha c_\alpha \lambda_\alpha \tag{13}$$

with *positive* coefficients

$$c_\alpha = (U \cdot V_\alpha^*)(U^* \cdot V_\alpha).$$

The normalization condition $(U \cdot U^*) = 1$ implies

$$\sum_\alpha c_\alpha = 1, \tag{14}$$

i.e., *the coefficient c_α provides the relative weight of the eigenmode V_α to the whole signal.*

Although the matrices R, A, and H are defined to be of infinite dimension, an exponential decrease of the elements $R_{m,m'}$ with m or m' allows one to truncate them to a finite dimension. It means that a small number of eigenvalues

[1] The initial density $\rho(\mathbf{r})$ may be set to the inverse of the domain volume V provided that eigenfunctions $u_m(\mathbf{r})$ are appropriately normalized.

λ_α and their weights c_α are in general sufficient to accurately describe the signal attenuation, whatever the geometrical complexity of the confining medium.

For a CPMG sequence, the same profile $\mathbf{g}(t)$ is periodically repeated n times, so that the amplitude of the nth echo (signal at time nT) can be also developed in a spectral decomposition:

$$S(nT) = (U \cdot H^n U^*) = \sum_\alpha c_\alpha \lambda_\alpha^n. \tag{15}$$

Consequently, the spectral properties of the matrix H determine *entirely* the amplitudes of the whole echo train. Since this matrix is Hermitian, the eigenvalues λ_α are real. On one hand, all eigenvalues should not exceed 1 to avoid an exponential growth of the echo amplitudes in Eq. (15). On the other hand, the diagonal-dominant structure of the matrix H would ensure that λ_α are positive,[2] i.e.

$$0 \leqslant \lambda_\alpha \leqslant 1. \tag{16}$$

These inequalities allow to identify the relation (15) as a *multiexponential attenuation of the echo amplitudes*

$$S(nT) = \sum_\alpha c_\alpha e^{-nT/\tau_\alpha} \tag{17}$$

with characteristic times

$$\frac{1}{\tau_\alpha} = \frac{1}{T} \ln \lambda_\alpha^{-1}. \tag{18}$$

The important point is that *such a multiexponential behavior is formally unavoidable, once a geometrical confinement is present*. At the same time, a reduction to a monoexponential attenuation can be observed under certain conditions which are examined in the next section.

4. CPMG measurements of restricted diffusion

In order to understand how a geometrical confinement leads to the multiexponential behavior, one can apply the above spectral analysis to simple domains for which the eigenfunctions $u_m(\mathbf{r})$ of the Laplace operator are known explicitly. We focus our attention to the restricted diffusion between two parallel infinite planes separated by distance $2a$, where the magnetic field gradient $\mathbf{g}(t)$ is applied in the normal direction to the planes. The problem is equivalent to one-dimensional diffusion on the interval $(0, 2a)$ with reflections at endpoints 0 and $2a$. A similar analysis will be then performed for diffusing nuclei confined inside an infinite cylinder (2D restriction) and a sphere (3D restriction).

[2] The rigorous mathematical demonstration of this property remains an open question. For this reason, we propose a physical argument. If some eigenvalues would be negative, the signal amplitudes for odd echoes would be systematically lower than that for even echoes. Such an oscillatory behavior due to parity of the echo number sounds unphysical, and has not been observed in experiment. Finally, we never found negative eigenvalues λ_α in numerical simulations for simple confining domains.

4.1. One-dimensional restricted diffusion

For this case, the eigenbasis of the Laplace operator is well known [34,35]:

$$\kappa_m = D(\pi m/2a)^2 \qquad u_m(x) = \epsilon_m\ (2a)^{-1/2} \cos(\pi m x/2a),$$

where $\epsilon_0 = 1$ and $\epsilon_m = \sqrt{2}$ for $m > 0$. The vector U and matrices A and R are calculated explicitly according to their definitions (9)–(12):

$$U_m = \epsilon_m \psi_m(\gamma \tau g(0)), \tag{19}$$

$$R_{m,m'} = \delta_{m,m'} \exp[-D\tau\pi^2 m^2/(2a)^2], \tag{20}$$

$$A_{m,m'}(q) = \epsilon_m \epsilon_{m'} \Big[\psi_{|m-m'|}(q) + \psi_{m+m'}(q)\Big] \Big/ 2, \tag{21}$$

where

$$\psi_m(q) = \frac{(-1)^m 2aq}{(2aq)^2 - (\pi m)^2} [\sin 2aq + i((-1)^m - \cos 2aq)]. \tag{22}$$

The last relation taken from the Callaghan's paper [28] differs by the phase factor e^{iaq} from that of Sukstanskii and Yablonskiy [31]. This distinction does not affect the signal $S(T)$ thanks to the rephasing condition (5).

Since the matrix H entirely determines the echo train attenuation, it should contain all relevant physical (i.e., dimensional) quantities of the problem: diffusion coefficient D, distance between planes $2a$, maximum gradient amplitude g, gyromagnetic ratio γ, and echo time T. However, as a mathematical object, the matrix H is independent of physical units. It means that the above physical quantities can enter only in dimensionless combinations. For this reason, we introduce two characteristic times: the diffusion time $t_d = a^2/D$ which determines the average time needed for a nucleus to diffuse on the distance a, and the dephasing time $t_c = (\gamma g a)^{-1}$ which defines the time of signal dephasing in the absence of diffusion. In other words, t_c is the time needed for dephasing of order 1 between two immobile nuclei within the distance a under gradient g. Looking at Eqs. (19)–(22), it is easy to check that the matrix H defined by (10) actually depends only on two independent dimensionless parameters T/t_d and T/t_c. Following [31], we also introduce their ratio

$$p = \frac{t_c}{t_d} = \frac{D}{\gamma g a^3}, \tag{23}$$

which may be formally ranged from 0 ("absence of diffusion") to infinity ("absence of gradient").

To calculate the signal attenuation for given values of two independent dimensionless parameters (e.g., p and T/t_c), the matrix H is computed numerically. For this purpose, the time interval is divided into N subintervals of duration $\tau = T/N$. Although the method can be applied for any gradient profile, a steady gradient is used for distinctness, i.e., the effective gradient is

$$\mathbf{g}(t) = \begin{cases} g & 0 \leqslant t < T/2, \\ 0 & t = T/2, \\ -g & T/2 < t \leqslant T. \end{cases}$$

In this case, the general definition (10) of the matrix H is reduced to

$$H = (RA)^{N/2-1} R (RA^*)^{N/2-1} R,$$

where

$$A \equiv A(\gamma\tau g) = A(N^{-1}(T/t_c)/a).$$

According to Eqs. (21) and (22), the elements of the matrix $A(q)$ are determined by the product qa. For this case, one gets $qa = N^{-1}(T/t_c)$ so that the matrix A depends only on the dimensionless parameter T/t_c (and numerical constant N^{-1}). In a similar way, the elements of the matrix R written as

$$R_{m,m'} = \delta_{m,m'} \exp\left[-N^{-1}(T/t_d)\pi^2 m^2/4\right]$$

show the dependence only on the dimensionless parameter $T/t_d = pT/t_c$.

The numerical analysis was implemented on the basis of Matlab software (the code can be sent under request). We have checked numerically that the time discretization of the gradient profile $N = 200$ and the truncation of the matrices A, R, and H to dimension 20×20 are fully enough to compute very accurately the signal $S(T)$ for the whole range of parameters used below.

4.2. Multiexponential behavior

The first numerical result confirms that only a small number of eigenmodes is sufficient to give a complete description of the signal attenuation. The dependence of the most contributing eigenvalues λ_α and their weights c_α on the normalized echo time T/t_c is shown in Fig. 2 for the case $p = 0.01$ (slow diffusion or high gradient).

The presence of several contributing eigenvalues leads to a multiexponential dependence of the time T_{cpmg} on the echo number n. If λ_1 denotes the largest eigenvalue for which $c_1 \neq 0$, the relation (3) can be written as

$$\frac{1}{T_{\mathrm{cpmg}}(n)} = \frac{1}{T}\ln\lambda_1^{-1} + \frac{1}{T}\ln\left[\frac{1 + \sum_{\alpha>1}\frac{c_\alpha}{c_1}\left(\frac{\lambda_\alpha}{\lambda_1}\right)^n}{1 + \sum_{\alpha>1}\frac{c_\alpha}{c_1}\left(\frac{\lambda_\alpha}{\lambda_1}\right)^{n+1}}\right]. \qquad (24)$$

If the condition

$$\lambda_\alpha \ll \lambda_1 \qquad (25)$$

was satisfied, the second term would be negligibly small for any n, and T_{cpmg} would be simplified to $T/\ln\lambda_1^{-1}$, characteristics of a classical monoexponential attenuation. However, this condition fails, at least for small echo times T, and T_{cpmg} becomes dependent on the echo number as shown in Fig. 3. For example, in the case $T = 10t_c$, the CPMG relaxation time ranges between $20t_c$ for the first

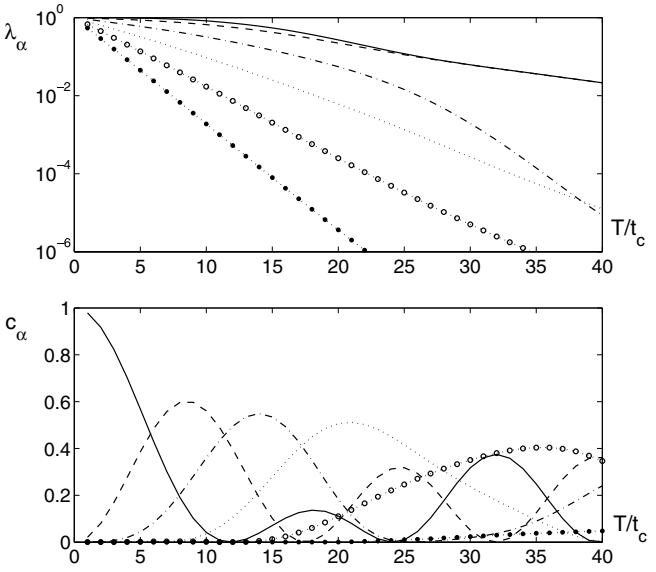

Fig. 2. The six most contributing eigenvalues λ_α (top) and their weights c_α (bottom) as a function of T/t_c at $p = 0.01$: $\alpha = 1$ (solid line), $\alpha = 2$ (dashed line) and $\alpha = 3$ (dash-dotted line), $\alpha = 4$ (dotted line), $\alpha = 5$ (dotted line with empty circles), and $\alpha = 6$ (dotted line with full circles).

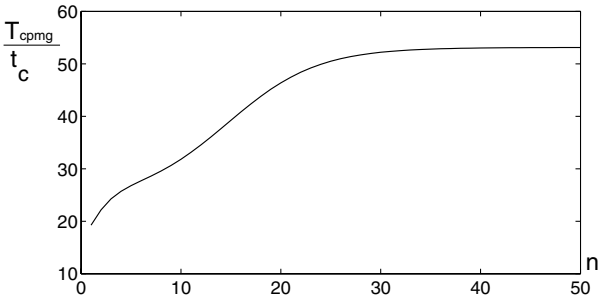

Fig. 3. CPMG relaxation time T_{cpmg} (in unit t_c) as a function of echo number n for $T = 10t_c$ at $p = 0.01$.

echoes and $53t_c$ for echo numbers larger than 30. The use of the classical relation (3) corresponding to a monoexponential fit would give thus different values of T_{cpmg} within this range depending on the number of echoes used to calculate it. Experimentally, it may be difficult or even impossible to overcome this bias by acquiring a large number of echoes sufficient to neglect the second term in (24) since it may be limited by short spin–spin relaxation time T_2 or small signal-to-noise ratio. As a practical consequence, one should pay particular attention to reliability of the CPMG measurements, once a geometrical confinement is relevant.

Yet, for very slow diffusion, when the parameter p is vanishing, the multiexponential behavior, intrinsic for diffusive motion in a confining medium, will not be apparent. In this trivial case, a very large number of echoes have to be acquired to eventually reveal a deviation from free diffusion. Such an almost unrestricted diffusion is out of the scope of the present paper.

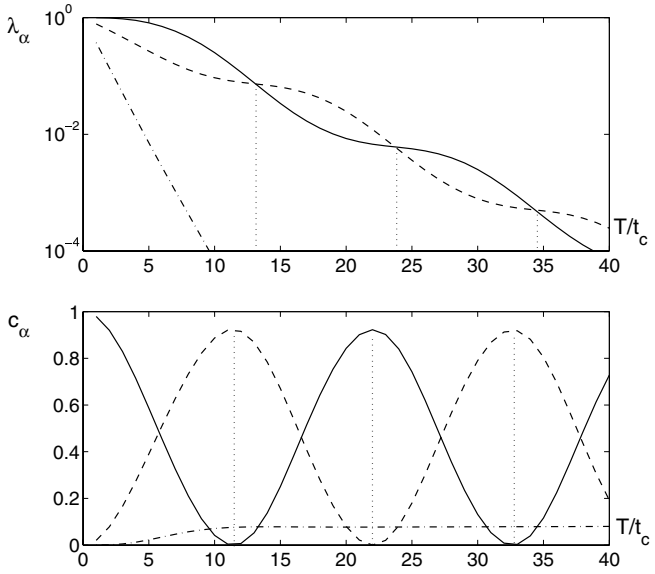

Fig. 4. The three most contributing eigenvalues λ_α (top) and their weights c_α (bottom) as a function of T/t_c at $p = 0.1$: $\alpha = 1$ (solid line), $\alpha = 2$ (dashed line), and $\alpha = 3$ (dash-dotted line).

4.3. Diffusive diffraction

For intermediate diffusion regime (higher p), the eigenvalues decrease more rapidly with echo time T, so that the number of contributing eigenmodes diminishes. For the case $p = 0.1$, only three eigenmodes are sufficient to calculate the signal attenuation, while the other eigenvalues are negligible. The dependence of the three most contributing eigenvalues λ_α and their weights c_α on the normalized time echo[3] T/t_c is shown in Fig. 4. The two largest eigenvalues, λ_1 and λ_2, exhibit *exponential decrease with almost periodic oscillatory modulations*, while the third eigenvalue λ_3 decreases more rapidly and without oscillations. The intersection points where $\lambda_1 = \lambda_2$ are almost equidistant and separated by time interval around $10t_c$. At the bottom of Fig. 4, one also finds the oscillatory behavior of the corresponding weights c_1 and c_2, while the third coefficient c_3 is constant for $T \gtrsim 10t_c$. The maxima of c_1 coincide with the minima of c_2 and vice versa in agreement with the normalization condition (14). These extrema are also separated by time interval around $10t_c$. Note that this period increases with p.

Such structural periodicity, very surprising at the first sight, resembles indeed *diffusive diffraction* for confining media in the limit of very fast diffusion [4]. However, the present situation is substantially different. First, it occurs when the diffusion time $t_d = t_c/p$ is greater (but not very much) than the dephasing time t_c that corresponds to an intermediate regime between slow and fast diffusion limits. Moreover, as one will see in the next subsection, this oscillatory behavior disappears in the fast diffusion regime. Second, there is no "q-space" related to the narrow pulse approximation [1] since we are working with a steady gradient. In fact, the observed periodicity concerns the contributing eigenvalues and their weights *as a function of the echo time T and not of the gradient amplitude g*. The oscillatory behavior is then transposed to the signal $S(T)$ via the spectral decomposition (13). This result opens a promising possibility to observe the diffusive diffraction even in such experimental conditions when the narrow pulse approximation is useless.[4]

The most unexpected result is that the intersection points for eigenvalues λ_1 and λ_2 do not coincide with the positions of extrema of the weights c_1 and c_2. This may lead to a kind of "resonant" dependence of the time T_{cpmg} on the echo time T. Let $T^{(1)}_{\min}$ denote the position of the first minimum of the weight c_1. As shown in Fig. 4, the condition $\lambda_1 > \lambda_2$ is satisfied for any $T \leqslant T^{(1)}_{\min}$, so that, for large enough n, one will observe a monoexponential decay with the relaxation time $\tau_1 = T/\ln \lambda_1^{-1}$. More rigorously, one has

$$\lim_{n\to\infty} T_{\mathrm{cpmg}}(n) = \tau_1.$$

When the echo time T slowly approaches $T^{(1)}_{\min}$, the weight c_1 of the most contributing eigenvalue λ_1 goes to 0, and one needs larger and larger n to reach the region where $T_{\mathrm{cpmg}}(n)$ becomes constant, τ_1. If T is chosen to be equal to $T^{(1)}_{\min}$, the eigenvalue λ_1 does not contribute any more ($c_1 = 0$), and the measured time T_{cpmg} is "switched" to the value $\tau_2 = T/\ln \lambda_2^{-1}$, i.e.,

$$\lim_{n\to\infty} T_{\mathrm{cpmg}}(n) = \tau_2.$$

Once the point $T^{(1)}_{\min}$ is passed, the contribution of the eigenvalue λ_1 re-appears, and the limit of $T_{\mathrm{cpmg}}(n)$ is again equal to τ_1. The sensitivity of the CPMG relaxation time to extrema of the weights c_α could be an interesting experimental tool to probe a complex geometry in the diffusive diffraction regime.

On the other hand, such sensitivity of the measured relaxation time T_{cpmg} to the timing of CPMG sequence (e.g., echo time T) may be a source of significant errors in experimental determination of physical characteristics like spin–spin relaxation time or diffusion coefficient. Indeed, if the echo time happened to be close to a minimum

[3] The knowledge of these spectral characteristics allows one to compute the spin echo signal $S(T)$ according to (13). Its variation with the echo time T was studied by Sukstanskii and Yablonskiy and shown in [31]. Our results precisely reproduce this dependence after rescaling the normalized echo time T/t_c by factor 2. We also checked its validity by the alternative Barzykin's approach [29,30].

[4] It should be noticed that, for the particular case of a steady gradient, the echo time T coincides with the gradient duration and can be thus thought, at least qualitatively, as a "measure" of the effective dephasing of the nuclei. To make this point more clear, we recall that the q-parameter is typically defined as $\gamma g\delta$, δ being the gradient duration. It means that the "strength" of the dephasing effect can be increased either by gradient amplitude g, or by its duration δ. Although such a simplified concept is formally appropriated only for the narrow pulse approximation ($\delta \to 0$), it seems to be meaningful in our case of a steady gradient.

of the weight c_1, the signal would be mainly determined by the second eigenmode so that T_{cpmg} would be close to τ_2 instead of τ_1. In this case, a small deviation of the echo time may change substantially the measured relaxation time. Since the minima of the weight c_1 as a function of T are a priori unknown, an improper choice of the echo time may lead to significant errors. A further theoretical investigation will be useful to give a quantitative criterion how the "proper" echo times should be chosen. In practice, the use of different echo times can be suggested in order to reduce this effect. In summary, the diffusive diffraction regime seems to be interesting to study complex morphologies due to the high sensitivity to different parameters, but it makes difficult a reliable quantitative determination of the physical characteristics like the diffusion coefficient. A monoexponential behavior would be more suitable for this purpose.

4.4. Monoexponential behavior

By further increasing the parameter p, the effects of diffusive diffraction gradually disappear. The time interval between two successive intersection points (when $\lambda_1 = \lambda_2$) and two successive extrema of their weights c_1 and c_2 increases and finally diverges as p approaches the critical value $p_c \simeq 0.44$. A similar behavior for the FID signal was first found by Sukstanskii and Yablonskiy [31]. For $p > p_c$, there is neither an intersection point nor an extremum. A typical dependence of the three most contributing eigenvalues and their weights on T/t_c is shown for $p = 0.5$ in Fig. 5. One finds that each eigenvalue decreases exponentially with progressively increasing slopes (and without oscillatory modulations). Their weights become constant

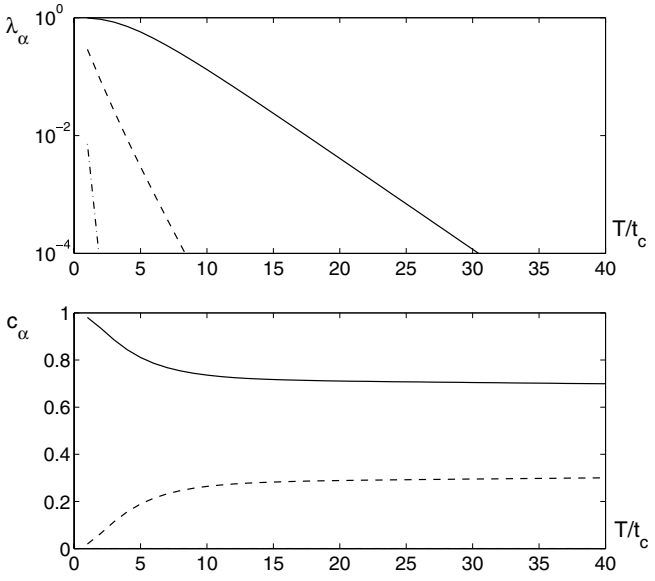

Fig. 5. The three most contributing eigenvalues λ_α (top) and their weights c_α (bottom) as function of T/t_c at $p = 0.5$: $\alpha = 1$ (solid line), $\alpha = 2$ (dashed line), and $\alpha = 3$ (dash-dotted line). The weight c_3 is too small to be visible at this scale.

for $T \gtrsim 10t_c$. Even for small T, the condition (25) is fulfilled so a monoexponential attenuation is expected with:

$$\frac{1}{T_{\mathrm{cpmg}}} = \frac{1}{T}\ln\lambda_1^{-1}$$

(the spin–spin relaxation can be taken into account by adding T_2^{-1} to the right-hand side of this expression).

For large enough p, the fast diffusion approximation [36] can be used to calculate the spin echo signal $S(T)$ and, consequently, the largest eigenvalue λ_1:

$$\lambda_1 \sim \exp\left[-\frac{\gamma^2 g^2 (2a)^4 T}{120D}\right] = \exp\left[-\frac{2}{15p}(T/t_c)\right]. \tag{26}$$

Such an exponential decrease of λ_1 as a function of T/t_c can be seen in Fig. 5, where the slope is found to be 0.347. Yet, this value remains 30% greater than the theoretical slope of $2/15p \simeq 0.267$. It shows that the fast diffusion approximation is not yet valid for $p = 0.5$. In the case $p = 1$, a slope of 0.133 is found, in very good agreement with the theoretical expression (26). The fast diffusion approximation becomes more and more precise with further increase of p.

The two last equations lead to the relaxation time for the fast diffusion:

$$\frac{1}{T_{\mathrm{cpmg}}} \simeq \frac{1}{T_2} + \frac{\gamma^2 g^2 (2a)^4}{120D}, \tag{27}$$

which greatly differs from the classical result (2) for free diffusion. Even if monoexponential attenuation is observed in a *confining medium* for a wide range of echo numbers, the relaxation time T_{cpmg} ought to be given by formula (27) for the fast diffusion regime and not by the classical equation (2), which is only valid for unrestricted diffusion. Once the motion of the nuclei is restricted, free diffusion results may remain relevant only for the first echoes.

4.5. Transition between two regimes

The above analysis showed the behavior of the largest eigenvalues and their weights as a function of the echo time T. One may also wonder how these spectral characteristics depend on the gradient amplitude g for a fixed echo time T. Since the dimensionless parameter p is inversely proportional to g, one may expect to observe a transition from the regime without oscillations for small g (large p) to the oscillatory regime for large g (small p). Such a transition should occur at gradient $g_c = D/(\gamma p_c a^3)$. Fig. 6 shows the two largest eigenvalues λ_1 and λ_2 and their weights c_1 and c_2 for a cubic cell of size $2a = 1$ mm filled of helium-3 ($\gamma \approx 2 \times 10^8$ rad T^{-1} s^{-1}, $D \approx 3$ cm^2/s at pressure 0.67 bar), in a steady gradient of duration $T = 10$ ms. In this case, the transition occurs around the gradient amplitude $g_c \approx 26.6$ mT/m. For gradient amplitudes smaller than g_c, one retrieves the fast diffusion approximation (26) for which $\ln\lambda_1$ is proportional to g^2. For larger gradient amplitude, λ_1 and λ_2 as well as c_1 and c_2 oscillate as expected.

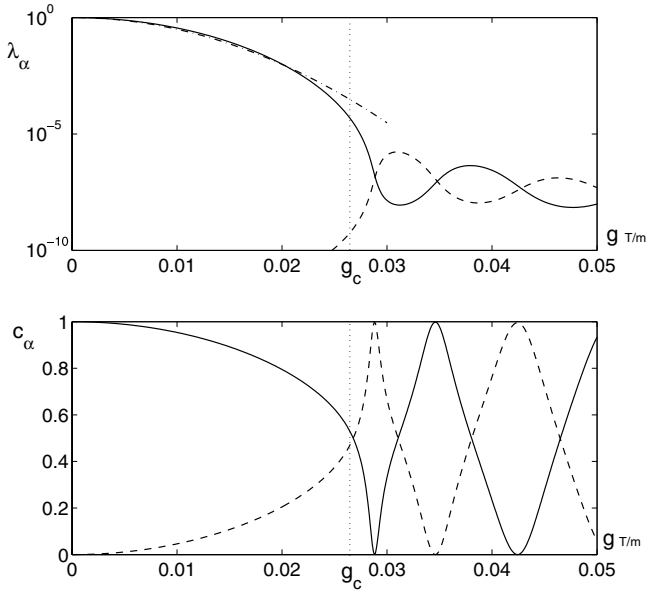

Fig. 6. The two largest eigenvalues λ_1 (solid line) and λ_2 (dashed line), top, and their weights c_1 and c_2, bottom, as a function of g for $D \approx 3\ \mathrm{cm}^2/\mathrm{s}$, $2a = 1$ mm and $T = 10$ ms. The fast diffusion approximation (27) for λ_1 is drawn by dash-dotted line. The dotted line shows the gradient $g_c \approx 26.6\ \mathrm{mT/m}$ corresponding to the critical parameter $p_c \simeq 0.44$. The third eigenvalue λ_3 is too small to be represented on this figure.

4.6. Application to realistic structures

Porous materials (e.g., cement) or biological tissues (e.g., mammal lungs) exhibit a complex geometrical structure with a variety of length scales. Although the multiple propagator approach and the present spectral analysis can be formally applied to study restricted diffusion in such media, the numerical calculation of the eigenfunctions $u_m(\mathbf{r})$ of the Laplace operator is still very difficult. Nonetheless, the initial NMR problem is reduced to an analysis of the spectral properties of the Laplace operator that is a long-standing and well-known problem in applied mathematics. A numerical computation of the contributing eigenvalues λ_α and their weights c_α for some realistic structures would help to answer some fundamental questions about restricted diffusion in realistic media. In particular, one could determine how many eigenmodes and relaxation times represent the signal attenuation, as well as what kind of oscillations or periodicity may occur. The dependence of the contributing eigenvalues on the physical parameters could be found.

Although such numerical results are not available yet, we may guess a general condition $p \gtrsim 1$ that ensures a monoexponential attenuation even for irregular geometry, where $2a$ denotes the characteristic length scale of the studied structure. In the case $p \ll 1$, a multiexponential behavior is expected. The intermediate values of the parameter p may be related to a diffusive diffraction which would be tightly related to a particular geometry.

5. Conclusion

An original theoretical aspect of restricted diffusion in confining media was discussed in the paper. To tackle the novel issue in a rigorous way, a spectral analysis was developed on the basis of the multiple propagator approach. A widely used monoexponential fit to the amplitude of periodically repeated spin echoes was called in question.

First, we have shown that a multiexponential attenuation of the CPMG multi-echo train occurs in any geometrically confined medium. A useful spectral representation in terms of eigenvalues λ_α for the echo amplitudes was derived. The relaxation times and their weights were related to physical parameters (diffusion coefficient, echo time, gradient profile, and gyromagnetic ratio) and geometrical characteristics (eigenbasis of the Laplace operator).

Second, we have applied the developed spectral analysis to study restricted diffusion in simple domains (two parallel planes, an infinite cylinder, and a sphere). For all these cases, it was shown that there were a small number of eigenvalues λ_α contributing to the echo amplitudes. Depending on the ratio p between the diffusion time t_d and the dephasing time t_c, three distinct regimes can be observed:

- In the case of fast diffusion or small gradient ($p > p_c$), each eigenvalue λ_α decreases exponentially with the echo time T, and the corresponding slope increases with α. As a consequence, the contribution to the spin echo signal of the largest eigenvalue is dominant that yields a monoexponential attenuation. The classical fast diffusion approximation allows one to relate the measured relaxation time to the physical parameters of the CPMG sequence.
- For the intermediate case ($p < p_c$), there are two major contributing eigenvalues λ_1 and λ_2 which still decrease exponentially, but also oscillate so to cross each other at nearly constant time intervals. Their weights c_1 and c_2 oscillate almost periodically which is a sign of diffusive diffraction. This behavior leads to a multiexponential attenuation with two different relaxation times.
- In the case of slow diffusion or high gradient ($p \ll 1$), several eigenmodes contribute to the signal, so that a complex multiexponential attenuation of the spin echo train is to be expected.

The transition between the first two regimes occurs at a critical value p_c which depends only on the geometry of the confining medium. In agreement with Sukstanskii and Yablonskiy [31], we found $p_c \simeq 0.44$ for one-dimensional restriction (diffusion between two parallel planes), $p_c \simeq 0.27$ for 2D (cylinder), and $p_c \simeq 0.18$ for 3D (sphere). For realistic structures, a similar distinction between monoexponential and multiexponential attenuation should be expected. Experimentally, the dimensionless parameter p can be used to check whether the use of a monoexponential fit to the acquired data is justified. A further numerical

study of the diffusive motion in realistic media is a promising perspective for the present spectral analysis.

Acknowledgments

The author is grateful to G. Guillot and X. Maître for valuable discussions on the subject and careful reading of the manuscript.

References

[1] P.T. Callaghan, Principles of Nuclear Magnetic Resonance Microscopy, Clarendon Press, Oxford, 1991.
[2] P.T. Callaghan, K.W. Jolley, J. Lelievre, Diffusion of water in the endosperm tissue of wheat grains as studied by pulsed field gradient nuclear magnetic resonance, Biophys. J. 28 (1979) 133.
[3] W.S. Price, P.W. Kuchel, Restricted diffusion of bicarbonate and hypophosphite ions modulated by transport in suspensions of red-blood-cells, J. Magn. Res. 90 (1990) 100.
[4] P.T. Callaghan, A. Coy, D. MacGowan, K.J. Packer, F.O. Zelaya, Diffraction-like effects in NMR diffusion studies of fluids in porous solids, Nature 351 (1991) 467.
[5] P.P. Mitra, P.N. Sen, L.M. Schwartz, P. Le Doussal, Diffusion propagator as a probe of the structure of porous medium, Phys. Rev. Lett. 68 (1992) 3555.
[6] D.J. Bergmann, K.-J. Dunn, Theory of diffusion in a porous-medium with applications to pulsed-field gradient NMR, Phys. Rev. B 50 (1994) 9153.
[7] M.D. Hurlimann, K.G. Helmer, T.M. de Swiet, P.N. Sen, C.H. Sotak, Spin echoes in a constant gradient and in the presence of simple restriction, J. Magn. Reson. A 113 (1995) 260.
[8] S.R. Wassall, Pulsed field-gradient-spin echo NMR studies of water diffusion in a phospholipid model membrane, Biophys. J. 71 (1996) 2724.
[9] H.E. Möller, X.J. Chen, B. Saam, K.D. Hagspiel, G.A. Johnson, T.A. Altes, E.E. de Lange, H.-U. Kauczor, MRI of the lungs using hyperpolarized noble gases, Magn. Reson. Med. 47 (2002) 1029–1051.
[10] E.J.R. van Beek, J.M. Wild, H.-U. Kauczor, W. Schreiber, J.P. Mugler, E.E. de Lange, Functional MRI of the lung using hyperpolarized 3-helium gas, J. Magn. Reson. Imaging 20 (2004) 540–554.
[11] H.Y. Carr, E.M. Purcell, Effects of diffusion on free precession in nuclear magnetic resonance experiments, Phys. Rev. 94 (1954) 630–638.
[12] S. Meiboom, D. Gill, Modified spin-echo method for measuring nuclear relaxation times, Rev. Sci. Instrum. 29 (1958) 688–691.
[13] Y.-Q. Song, S. Ryu, P.N. Sen, Determining multiple length scales in rocks, Nature 406 (2000) 178.
[14] W.P. Halperin, J.Y. Jehng, Y.Q. Song, Application of spin–spin relaxation to measurement of surface area and pore size distributions in a hydrating cement paste, Magn. Reson. Imaging 12 (1994) 169.
[15] N. Nestle, P. Galvosas, O. Geier, M. Dakkouri, C. Zimmermann, J. Karger, NMR studies of water diffusion and relaxation in hydrating slag-based construction materials, Magn. Reson. Imaging 19 (2001) 547.
[16] A. Plassais, M.P. Pomies, N. Lequeux, P. Boch, J.-P. Korb, D. Petit, F. Barberon, Micropore size analysis by NMR in hydrated cement, Magn. Reson. Imaging 21 (2003) 369.
[17] M. Gussoni, F. Greco, F. Bonazzi, A. Vezzoli, D. Botta, G. Dotelli, I. Natali Sora, R. Pelosato, L. Zetta, ^{1}H NMR spin–spin relaxation and imaging in porous systems: an application to the morphological study of white portland cement during hydration in the presence of organics, Magn. Reson. Imaging 22 (2004) 877.
[18] E. Durand, G. Guillot, L. Darrasse, G. Tastevin, P.J. Nacher, A. Vignaud, D. Vattolo, J. Bittoun, CPMG measurements and ultrafast imaging in human lungs with hyperpolarized helium-3 at low field (0.1 T), Magn. Reson. Med. 47 (2002) 75–81.
[19] J. Vanbrake, P.M. Heertjes, Analysis of diffusion in macroporous media in terms of a porosity, a tortuosity and a constrictivity factor, Int. J. Heat Mass Transfer 17 (9) (1974) 1093–1103.
[20] C.T. Wang, J.M. Smith, Tortuosity factor for diffusion in catalyst pellets, AIChE J. 29 (1) (1983) 132–136.
[21] N. Epstein, On tortuosity and the tortuosity factor in flow and diffusion through porous media, Chem. Eng. Sci. 44 (3) (1989) 777–779.
[22] P.N. Sen, L.M. Schwartz, P.P. Mitra, Probing the structure of porous-media using NMR spin echoes, Magn. Reson. Imaging 12 (2) (1994) 227–230.
[23] K.G. Helmer, B.J. Dardzinski, C.H. Sotak, The application of porous-media theory to the investigation of time-dependent diffusion in vivo systems, NMR Biomed. 8 (7–8) (1995) 297–306.
[24] R.A. Garza-Lopez, L. Naya, J.J. Kozak, Tortuosity factor for permeant flow through a fractal solid, J. Chem. Phys. 112 (22) (2000) 9956–9960.
[25] P.N. Sen, A. André, S. Axelrod, Spin echoes of nuclear magnetization diffusing in a constant magnetic field gradient and in a restricted geometry, J. Chem. Phys. 111 (1999) 6548.
[26] A.A. Maudsley, Modified Carr–Purcell–Meiboom–Gill sequence for NMR fourier imaging applications, J. Magn. Reson. 69 (1986) 488–491.
[27] A. Caprihan, L.Z. Wang, E. Fukushima, A multiple-narrow-pulse approximation for restricted diffusion in a time-varying field gradient, J. Magn. Reson. A 118 (1996) 94.
[28] P.T. Callaghan, A simple matrix formalism for spin echo analysis of restricted diffusion under generalized gradient waveforms, J. Magn. Res. 129 (1997) 74.
[29] A.V. Barzykin, Exact solution of the Torrey–Bloch equation for a spin echo in restricted geometries, Phys. Rev. B 58 (1998) 14171.
[30] A.V. Barzykin, Theory of spin echo in restricted geometries under a step-wise gradient pulse sequence, J. Magn. Reson. 139 (1999) 342.
[31] A.L. Sukstanskii, D.A. Yablonskiy, Effects of restricted diffusion on MR signal formation, J. Magn. Reson. 157 (2002) 92.
[32] S.L. Codd, P.T. Callaghan, Spin echo analysis of restricted diffusion under generalized gradient waveforms: planar, cylindrical and spherical pores with wall relaxivity, J. Magn. Reson. 137 (1999) 358.
[33] G.B. Arfken, H.J. Weber, Mathematical Methods for Physicists, fifth ed., Academic Press, San Diego, 2001.
[34] J. Crank, The Mathematics of Diffusion, Oxford University Press, Oxford, 1956.
[35] H.S. Carslaw, J.C. Jaeger, Conduction of Heat in Solids, second ed., Oxford University Press, Oxford, 1959.
[36] B. Robertson, Spin-echo decay of spins diffusing in a bounded region, Phys. Rev. 151 (1) (1966) 273.